

# Focusing and reversal of surface acoustic waves propagating on a sphere

D. Clorennec and D. Royer

Laboratoire Ondes et Acoustique, Université Paris 7 - CNRS UMR 7587

ESPCI - 10, rue Vauquelin, 75231 Paris Cedex 05- France

Email : dominique.clorennec@loa.espci.fr

## Abstract

Using the laser ultrasonic technique, we investigate the propagation of spherical surface acoustic waves (SSAW). A finite thermoelastic line source gives rise to combined focusing and reversal effects. As for propagation on a cylinder, the reversal of the SSAW pulse is explained by the dispersion of the high frequency components of the laser-generated acoustic pulse. The focussing effect, due to the curvature of the surface, depends on the angular aperture of the source. Optimal conditions for diffraction free propagation are derived, both in harmonic and pulse regimes.

Surface acoustic waves (SAW) propagating on a sphere have characteristics different from those of Rayleigh waves propagating on a plane. They have been studied by geophysicists [1,2]. First experiments where the waves were generated by a pulsed YAG-laser and detected by an optical heterodyne probe demonstrated the advantages of laser-based ultrasonic techniques [3,4]. Recently divergent, focused, and collimated spherical SAW were excited by an interdigital transducer [5].

In a previous work [6], we show that a short SAW pulse was reversed during its propagation on a duraluminum or a steel cylinder. This phenomena was explained by the dispersion effect on the large  $ka$  components ( $k$ : SAW wave number,  $a$ : cylinder radius). In this paper, using the non-contact laser ultrasonic technique, we investigate the combined focusing and reversal effects for spherical surface acoustic waves (SSAW).

As for a cylinder, SSAW fall in two categories: the Rayleigh and the so-called whispering gallery waves, related to bulk acoustic waves. The dispersion equation providing the angular frequency  $\omega$  versus the wave number  $k$  is given in reference [2]. In our experiments only the Rayleigh mode, giving rise to large surface displacements, is efficiently coupled to the pulsed laser source and to the interferometric laser probe. Figure 1 shows, for a steel sphere of radius  $a$ , the Rayleigh wave phase velocity  $V$  versus the product  $ka$ . The dispersion effect is mostly noticeable for low frequencies ( $ka < 10$ ) such that the wavelength  $\lambda$  is larger than  $a/2$ . As  $ka$  tends to infinity (large frequencies), the velocity tends to the value  $V_R = 2960$  m/s corresponding to the speed of the Rayleigh wave in a thick steel plate. Since this behaviour is similar to that of Rayleigh wave propagating on a cylinder, a reversal of the mechanical displacement is expected for a given longitude angle  $\phi$  [6].

Experiments were carried out on a steel sphere of diameter 50 mm. Surface waves were generated by a Nd:YAG laser providing pulses having a duration  $\Delta = 20$  ns and a 3-mJ energy.

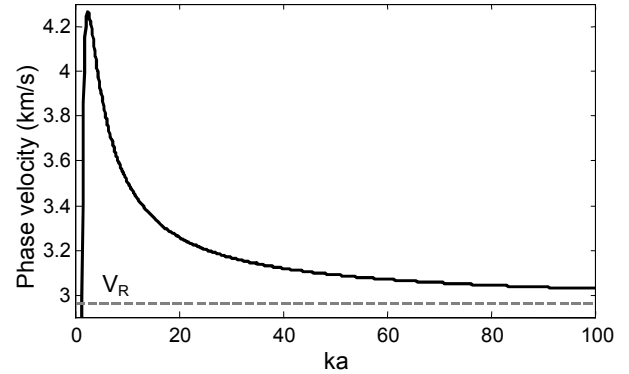


Fig. 1 : Rayleigh wave phase velocity versus  $ka$  for a steel sphere of radius  $a$ .

A beam expander and a cylindrical lens were used to focus the beam onto a line along the meridian  $\phi = 0^\circ$  (fig. 2). The spatial energy distribution, plotted by scanning a narrow slit, was closed to a Gaussian. The full length  $2b$  of the thermoelastic source was defined at  $1/e$  of the maximum value. The SSAW's propagate along an equator of the sphere perpendicular to the source. The mechanical displacement normal to the surface was measured by a heterodyne interferometer (detection bandwidth : 50 kHz - 20 MHz) equipped with a 100-mW continuous laser emitting at 532 nm [7]. The first arrival of the Rayleigh wave was recorded according to the angle  $\phi$  between the source and the detection point.

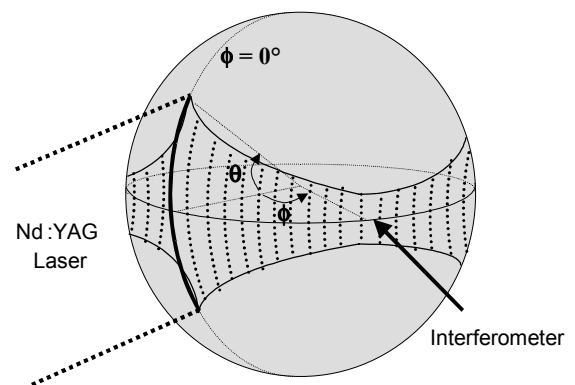


Fig. 2 : Rayleigh waves a sphere. The waves are generated by a pulsed YAG laser focused onto a line of length  $2b$ . They are detected by an optical heterodyne interferometer.

Figure 3 shows a series of wave forms from  $\phi = 20^\circ$  to  $\phi = 180^\circ$  (step  $5^\circ$ ) launches by a line source of length  $2b = 12$  mm. In the vicinity of  $\phi = 90^\circ$  two phenomena are observed: the displacement is reversed and the amplitude of the SAW

pulse undergoes a maximum. As for a cylinder, the first effect can be explained by the dispersion of the high frequency components (Eq. 8 of Ref. 6).

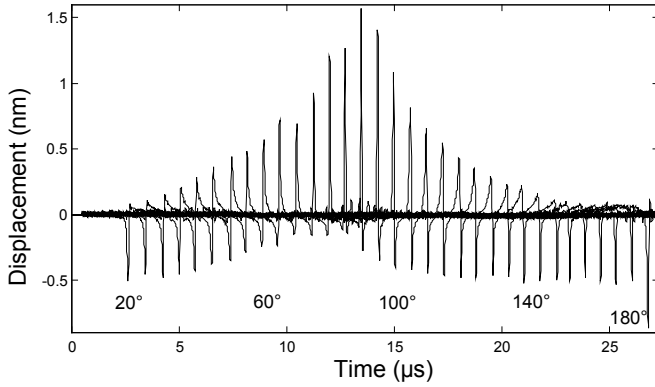


Fig. 3 : Line source of length  $2b = 12$  mm on a steel sphere of radius 25-mm. Rayleigh wave forms recorded along the equator from  $20^\circ$  to  $180^\circ$  ( $5^\circ$  step).

Fitting the tail of the dispersion curve in Fig. 1 ( $ka > 100$ ) with a function

$$V = V_R \left(1 + \frac{\varepsilon}{ka}\right) \quad (1)$$

leads for the parameter  $\varepsilon$  to a value 2.22 which gives a reversal angle  $\phi_r = \pi/\varepsilon = 81^\circ$  closed to the experimental figure ( $83^\circ$ ). The second effect is due to the curvature of the surface: the Rayleigh wave converges towards the point on the equator located at  $\phi = 90^\circ$ . The profile of the SAW beam was measured by scanning the optical probe beam perpendicularly to the equator at  $\phi = 90^\circ$ . Compared to the source length, the beam compression factor is equal to 3.5. If this focusing effect is compensated by normalising the amplitude of the SAW pulses in Figure 3, the Rayleigh waveform variation is similar to that obtained in the case of a cylinder (fig. 3 of Ref. 6).

As pointed out by Tsukahara *et al* [8], a collimated Rayleigh wave of nearly constant width can propagate around the equator if the length  $2b = 2a\theta$  of the source is appropriately chosen.

In time harmonic regime, the finite angular aperture  $2\theta$  of the line makes the Rayleigh wave to spread in a cone of angle  $\alpha$  such that:  $\sin \alpha = \lambda_R/b$ . The curvature of the line source tends to focus the Rayleigh beam into a cone of angle  $\beta$  such that  $\sin \beta = 2b/F$ , where the focal length  $F$  is equal to  $\pi a/2$ . The two effects balance when the diverging and converging angles  $\alpha$  and  $\beta$  are equal. The aperture angle  $\theta_{col}$  for launching a collimated beam expressed by the equation:

$$\theta_{col} = \sqrt{\frac{\pi \lambda_R}{4a}} \cong 1.25 \sqrt{\frac{\lambda_R}{2a}} \quad (2)$$

In pulse regime, the acoustic beam can be focussed only if the focal zone lies in the near field domain. For a Gaussian thermoelastic source, this condition expressed as (Eq. 23 of ref. 9):

$$F = \frac{\pi}{2} a \leq \frac{b^2}{V_R \Delta} \quad (3)$$

The equality corresponds to a collimated beam of constant angular aperture

$$\theta_{col} = \sqrt{\frac{\pi}{2} \frac{V_R \Delta}{a}} \cong 1.25 \sqrt{\frac{V_R \Delta}{a}} \quad (4)$$

In our experimental conditions ( $\Delta = 20$  ns,  $a = 25$  mm,  $V_R = 2960$  m/s), diffraction free propagation is obtained for  $\theta_{col} = 3.5^\circ$  and an optimal source length

$$2b_{col} = \sqrt{2\pi a V_R \Delta} \quad (5)$$

equal to 3.05 mm. Figure 4 shows the results of an experiment performed with a line source of length  $2b = 3$  mm. As expected, the amplitude of the Rayleigh pulse is nearly constant. No focussing effect is observed at  $\phi = 90^\circ$ .

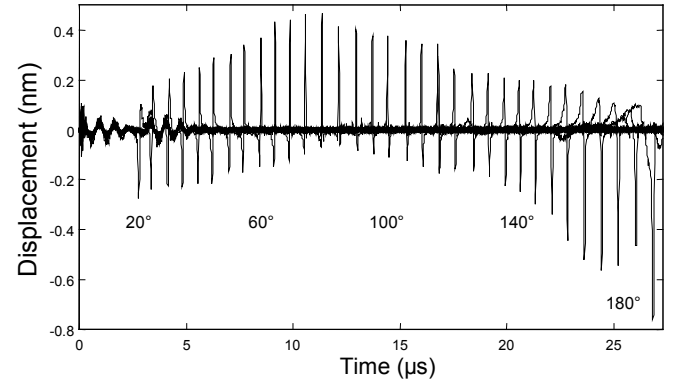


Fig. 4 : Line source of length  $2b = 3$  mm on a steel sphere of radius 25-mm. Rayleigh wave forms recorded along the equator from  $20^\circ$  to  $180^\circ$  ( $5^\circ$  step).

In conclusion, experimental and theoretical investigations of spherical surface acoustic waves generated by a thermoelastic line source show that the mechanical displacement is periodically reversed and focussed. The origin of the first effect is the same that for a cylinder. The second effect due to the surface curvature is specific to the sphere. For time harmonic and pulsed regimes, geometrical conditions for launching a collimated SSAW beam have been derived and experimentally observed.

## References

- 1 K. Sezawa, Bull. Earthquake Res. Inst. (Tokyo) **2**, 21 (1927)
- 2 Y. Sato and T. Usami, Geophys. Mag., **31**, 15 (1962)
- 3 D. Royer, E. Dieulesaint, X. Jia, and Y. Shui, Appl. Phys. Lett., **52**, 706 (1988).
- 4 Y. Shui, D. Royer, E. Dieulesaint and Z. Sun, 1998 IEEE Ultrasonics Symposium Proc. (IEEE, New York, 1988) p. 343.
- 5 S. Ishikawa, N. Nakaso, N. Takeda, T. Mihara, Y. Tsukahara and K. Yamanaka, Appl. Phys. Lett., **83**, 4649 (2003).
- 6 D. Clorennec and D. Royer, Appl. Phys. Lett., **82**, 4608 (2003)
- 7 D. Royer, 1995 World Congress on Ultrasonics Proc., p. 51 (1995).
- 8 Y. Tsukahara, N. Nakaso, H. Cho and K. Yamanaka, Appl. Phys. Lett., **77**, 2926 (2000).
- 9 D. Royer and C. Chenu, Ultrasonics, **38**, 891 (2000).